The 21st International Congress on Sound and Vibration

13-17 July, 2014, Beijing/China

PROPELLER RADIATED NOISE DUE TO WAKE FIELD OF THE SHIP BASED ON CFD, FEM AND BEM

Mohamed Bennaya,Wenping Zhang and Yipeng Cao

College of power and energy engineering, Harbin Engineering University, Harbin, China

bennaya_m@yahoo.com

Moutaz M. Hegaze

MTC, Cairo, Egypt

The low frequency structural and acoustic responses of a 4-bladed propeller due to fluctuating forces induced as a result of propeller-bulk carrier interaction at full scale have been investigated for the first time. Firstly, the ship, propeller and propeller-ship models have been independently built and validated via computational fluid dynamics (CFD) at model scale. Secondly, the propeller-ship model has been scaled and unsteady simulation has been done to extract the induced distributed forces on the propeller surface nodes using CFD. Thirdly, structural and acoustic responses are predicted using finite element method (FEM) and boundary element method (BEM) in the time domain. The results show some new contributions (1) the structural and acoustic responses are mainly tonal at the fundamental frequency of the propeller's structure. (2) Related to the responses due to the propeller exciting forces, the highest acoustic response occurs at the first harmony of the propeller speed among the all harmonies including the blade passing frequency. (3) The sound pressure radiated due to vertical and transverse forces are smaller than the radiated one due to the axial force (thrust), which is almost the same sound pressure radiated due to total forces. This method will enable the researchers to monitor the structural and acoustic responses at propeller rotating speeds and at the structural modes of the propeller which are not investigated before.

1. Introduction

The induced periodic hydrodynamic exciting forces on the propeller and its individual blades due to the propeller-hull interaction are the underlying cause of the propeller noise in non-cavitating condition, since it can induce vibration in the propeller it self or transmitted through the shaft and bearings to the hull structure.

Nowadays, many researchers are trying to investigate this issue, Wei et al. [1] and Wei and Wang [2] numerically investigated the acoustic response of submarine structure due to propeller excitation. They considered the propeller as a rigid body by modelling it in the FEM as a concentrated mass subjected to a concentrated exciting force which calculated as a resultant force from the propeller surface nodes via CFD. Despite these studies are very useful, but they lack the accuracy for two reasons. The first one, the calculation of the resultant periodic forces of the propeller through CFD neglected the propeller excitation at propeller speed *n* due to the phase cancellation of the blade forces. The second one, however they calculated the excitation due to propeller, they completely neglect it as a 3-D elastic structure. So, it is normal in their results to find out that, there is no acoustic response at propeller speed *n* and at the propeller structural modes.

On the other hand some researchers studied the same issue without using CFD to calculate the exciting force. In their works they used FEM and BEM only. Some of these studies include Li et al. [3] and Cao et al. [4], in these works, the propeller exciting forces are simulated as a unit pulse force applied

on the concentrated mass. However these works are quite useful, but they also completely neglect the acoustic response at propeller speed n and BPF, which showed have an acoustic response higher than that due to the global modes of the ship (Wei and Wang [2]). In addition they neglected also the propeller structural modes because they simulated it as a concentrated rigid mass.

In this work, the previous short comings are cured. The following assumptions are used: (1) the damping effect of the material is neglected. (2) Wei and Wang [2] concluded that, the contributions of the exciting forces are higher than that of the hull structural modes. So, the ship 3-D structure is only included in CFD and excluded in the FEM and BEM for the sake of computational time consumption. (3) The original point of the coordinates is fixed on the centre of the propeller.

2. Steady hydrodynamics of independent ship hull

Ship model No.S00905P-A has been designed in Shanghai Ship and Shipping Research Institute (SSSRI) as a model for a 35000DWT bulk carrier with scale ratio $\lambda = 29.197$ as shown in

Figure 1. ANSYS-ICEM V13 has been used to generate the mesh for the ship model computational domain shown in Table 1. Where L_{wl}, T and B are respectively length on waterline, draft and breadth of the ship model. An unstructured mesh was employed for grid generation around the model hull and structured mesh was employed for the rest of the computational domain as shown in Figure 2.

Figure 1. Bulk Carrier 35000DWT hull form with fore and aft drafts equal to 9.5 m.

The hull is modelled using a no-slip wall condition and RNG k-epsilon turbulence model has been used. The air resistance has been neglected through considering the water surface as symmetric surface. Inlet velocity is defined at one waterline length upstream of the hull with inlet turbulent intensity and viscosity ratio equal to 2 %. Pressure outlet is positioned 5 waterline lengths downstream of the hull. The simulations are supposed to be converged when the residual is below 10^{-5}. The final mesh for the ship model contains a total No. of 1.8 M elements.

Table 1. Global domain dimensions (distance is measured from frontal tip of the hull).

Inlet boundary	Outlet boundary	Height	Width
L_{wl}	5 L_{wl}	7 T	5 B

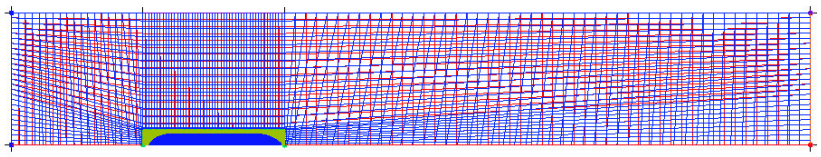

Figure 2. Ship resistance computational grid.

The total resistance of the ship model R_{tm} has been calculated via CFD for various model speeds. Then the ship model resistance coefficient $C_{tm} = \dfrac{R_{tm}}{0.5\rho S_m V_m^2}$ has been calculated, where V_m, S_m and ρ are respectively velocity, wetted surface area and water density. The obtained numerical results agree well with the experimental data as shown in Figure 3.

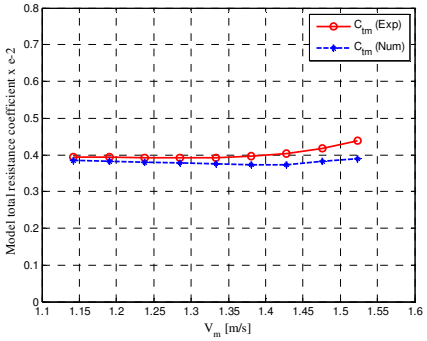

Figure 3. Ship resistance coefficient at T =9.5 m.

3. Steady hydrodynamics of independent propeller

The experimental open water hydrodynamic characteristics have been performed in SSSRI for the model scale propeller with $\lambda = 29.197$. ANSYS-ICEM V13 has been used to generate the mesh for the propeller computational domain shown in Figure 4.

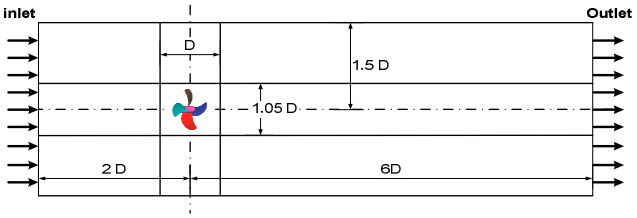

Figure 4. Scheme of propeller computational domain for steady analysis.

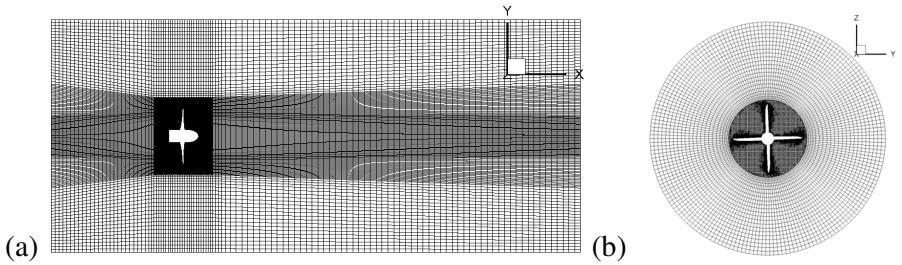

Figure 5. Propeller computational grid (a) Mesh at plane z=0. (b) Mesh at plane x=0.

A representative example of the computational grid is given as shown in Figure 5. The final mesh model contains a total No. of 1.8 M elements. The y^+ value represents a non-dimensional distance of the first node from the wall and this value is important to properly model the turbulence boundary layer. The y^+ value on the boundary of the propeller blades is calculated, and its value was found to be in the recommended range $30 < y^+ < 500$. The inlet velocity is set to be equal to the advance velocity V_m along x direction at the inlet and the pressure outlet is considered at the outlet. No slip conditions are used on the blades and the hub. The simulations are supposed to be converged when the residual is below 10^{-5}. The propeller advance coefficient $J = \dfrac{V_m}{n_m D_m}$ changed from 0.1 to 0.7, where n_m and D_m are respectively the propeller rotating speed and diameter at model scale. Finally the thrust coefficient K_T, torque coefficient K_Q, and the efficiency coefficient η are evaluated via

CFD, with $K_T = \frac{T}{\rho n_m^2 D_m^4}$, $K_Q = \frac{Q}{\rho n_m^2 D_m^5}$ and $\eta = \frac{K_T}{K_Q}\frac{J}{2\pi}$, where T and Q are respectively the propeller's thrust and torque. RNG K-epsilon is chosen as the turbulence model. The values for K_T and K_Q agree well with the experimental data whilst the open water efficiency slightly differs at high advance coefficient as shown in Figure 6.

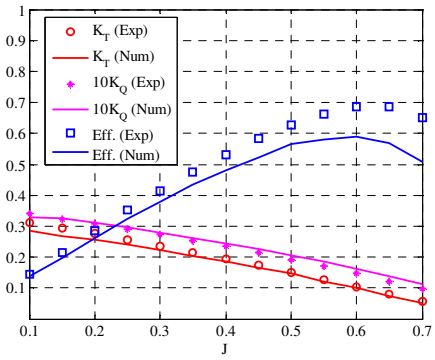

Figure 6. Propeller open water characteristics.

4. Hydrodynamic characteristics of propeller-hull interaction

The propeller and the ship models were combined together to perform the steady simulation with RANS equations. Propeller's thrust and torque have been computed and compared with the experimental data of the self propulsion test of the ship model provided by SSSRI. Small zone of computational domain including the hull and the propeller with dimension (1.1L_{wl}, 1.1B, 1.1T) has been established, unstructured mesh has been used to mesh this small zone and the structured mesh has been used for the rest of the computational domain as shown in Figure 7.

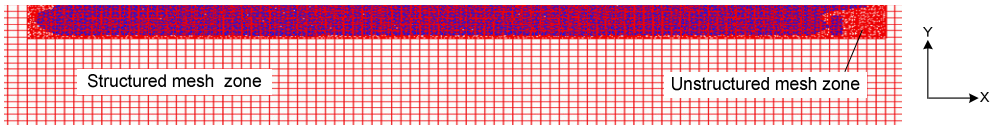

Figure 7. Generalized mesh for numerical solution of propeller-hull interaction model.

(a) 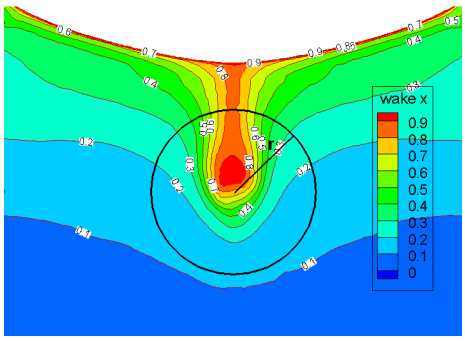

(b) 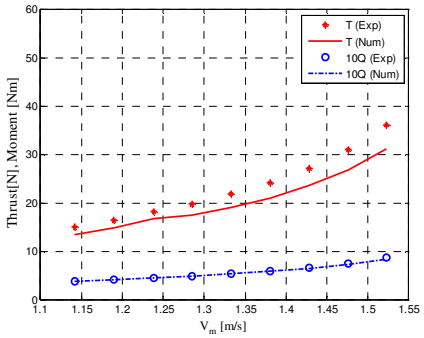

Figure 8. Numerical results (a) axial nominal wake with $V_m = 1.304$ m/s at plane x=0. (b) propeller thrust and torque.

The computed results for T and Q due to the wake field of the bulk carrier ship shown in Figure 8(a) are as shown in Figure 8(b). The numerical results agree well with the experimental data whilst for the thrust force slightly differs at high velocity. Where r is the radius of the propeller disk.

5. Propeller hydrodynamic exciting forces at full scale

After the validation of the propeller-hull interaction at model scale, the model is scaled to full scale and unsteady RANS simulations have been used via FLUENT software to calculate the induced 3-D hydrodynamic forces of the propeller. Propeller speed (n_s) and ship speed (V_s) at full scale were set to be 1.7 rps and 6.94 m/s respectively, which are corresponding to the operating speed of the ship 13.5 Kn. Sliding mesh technique and SST (Shear Stress Transport) k-omega turbulence model have been used.

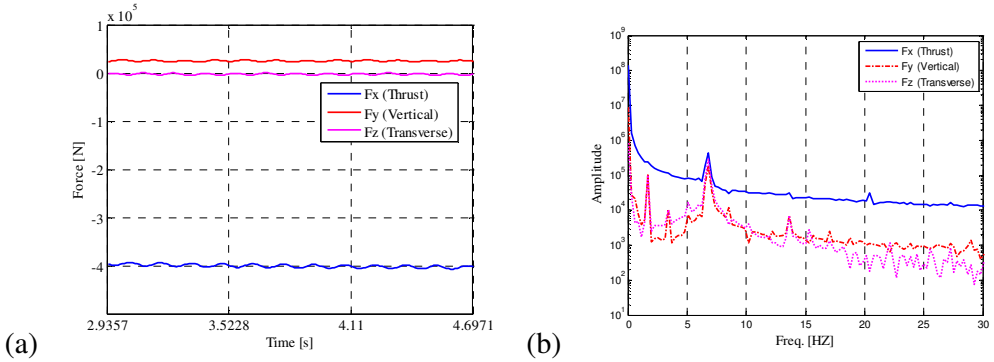

(a) (b)

Figure 9. Propeller's blades hydrodynamic periodic forces *Fx*, *Fy* and *Fz* at $n_s = 1.7$ rps (a) in time domain (b) in frequency domain.

As shown in Figure 9, *Fx* dominates the frequency domain and the response's maximum peaks for all forces exist at speed equal the blade passing frequency (BPF). Here , $\mathrm{BPF} = n_s * z$ (Hz), where z is the blades number of the propeller. And this attributed to the phase cancellation between all blades when the resultant force for all blades in each direction is computed as a concentrated force. So, the contribution of the forces at n_s and its multiplication are low. Moreover, it is vanished related to *Fx*. On the other hand, *Fy* and *Fz* have strong existance (peaks) at speed=n_s .

6. Full scale propeller FEM

In this section, the 3-D computational grid for propeller finite element model is built with the same surface 2-D grid of the CFD with HYPERMESH software. So, surface nodes distribution is the same for both CFD and FEM calculations (nodes are coincident). As a consequence high accuracy is guaranteed. On the other hand, the forces of the surface nodes extracted from propeller's CFD at full scale model through the time history of the unsteady calculations could be applied on the propeller FEM to get the structural and acoustic responses due to these applied forces. ANSYS software is used to calculate the structural response of the propeller due to the exciting distributed force on the propeller nodes surface calculated with CFD. Propeller 3-D structure is modelled with ETSOLID45, one way fluid structure interaction (FSI) is considered by ETFLUID30 element, a representative example for one blade FEM with FSI surface is shown in Figure 10 (a).

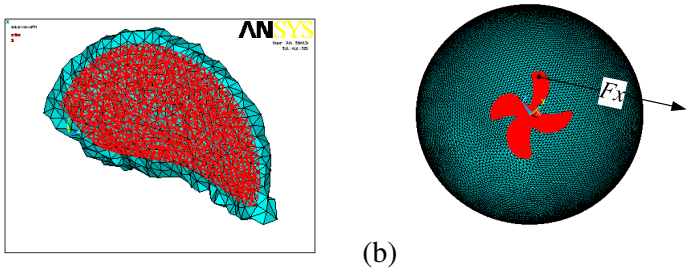

(a) (b)

Figure 10. Propeller FEM with FSI (a) one blade (b) final computational domain.

Finally, the propeller FEM with FSI for vibration analysis has been built as shown in Figure 10 with final mesh model contains a total No. of 512601elements and total No. of 88963 nodes. The propeller modal analysis has been done and the propeller fundamental damped frequency $\omega_1 = 25.37$ Hz.

6.1 Propeller FE transient response

The transient response for the propeller at full scale has been calculated. The forces on the propeller surface nodes (14879 nodes) have been extracted from CFD with time step 0.01 s. Then these forces have been applied at the same nodes in the propeller FEM. A representative example of an applied force *Fx* history at the selected node shown in Figure 10(b) is as shown in Figure 11(a). The harmonic exciting force *Fx* is mainly tonal with propeller speed n_s and its multiplications with maximum peak at n_s as shown in Figure 11 (b).

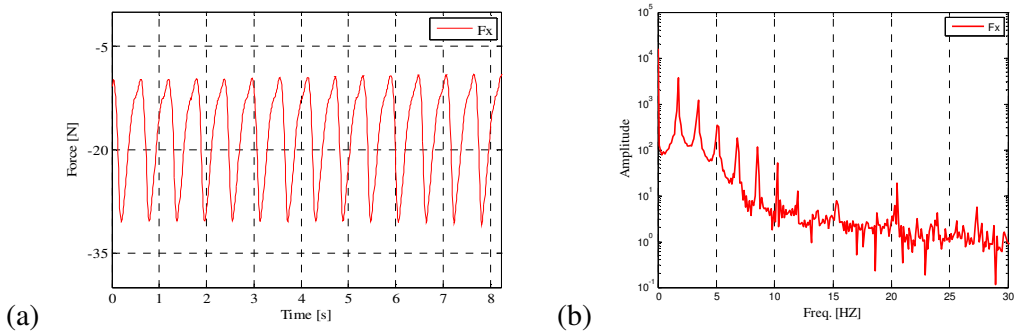

Figure 11. The applied force history of the propeller surface at the selected node (Figure 10(b)) in *x* direction, n_s=1.7 rps extracted from CFD (a) in time domain (b) in frequency domain.

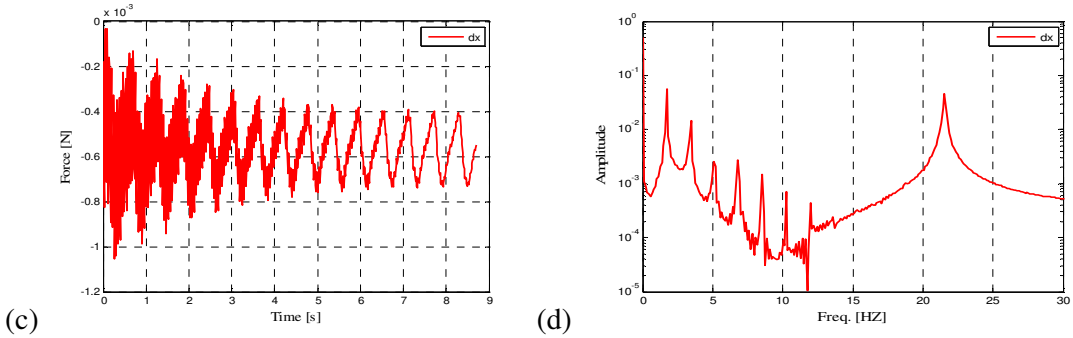

Figure 12. Transient response of the propeller in *x* direction at the selected node, n_s=1.7 rps (a) in time domain (b) in frequency domain.

The responses of the propeller are independently calculated due to the applied forces *Fx*, *Fy* and *Fz*. After that, all forces are applied to investigate the whole effect. A representative example of the propeller structural response due to the applied force shown in Figure 11 is as shown in Figure 12. The time domain shown in Figure 12 (a) is split to transient and steady state regions. Such this transient region is attributed to the computational time required from the applied harmonic forces to overcome the propeller inertia, after that the response changes to the steady state. The responses at the 1st harmony of propeller speed and the fundamental frequency are higher than that at PBF, which it is not known before. It should be marked that, according to the propeller modal analysis, $\omega_1 = 25.377$ Hz, however the transient response due to the harmonic exciting force shows that resonating frequency equal 21.58 Hz. And this is attributed to, the maximum steady state response of the damped vibration due to harmonic force occurs when,

$$\omega_m = \omega_d \frac{\sqrt{1-2\zeta^2}}{\sqrt{1-\zeta^2}} \tag{1}$$

Where ω_m , ω_d and ζ are respectively the maximum response frequency, damped natural frequency and damping ratio, this means that, ω_m is lower than ω_d with certain ratio according to the damping effect of the water (Rao [5]).

7. Underwater acoustic response of the propeller

LMS virtual Lab11 has been used to calculate the acoustic response of the propeller due to the hydrodynamic exciting forces of propeller-ship interaction using acoustic transient boundary element method (BEM). Two monitoring positions are defined in plane x=0, the first one represents a near field point and the second one represents a far field point at distance D_s and $10D_s$ respectively down the propeller centre. Where D_s is the propeller diameter at full scale. Reference sound pressure is set to be $1e^{-6}$ Pa.

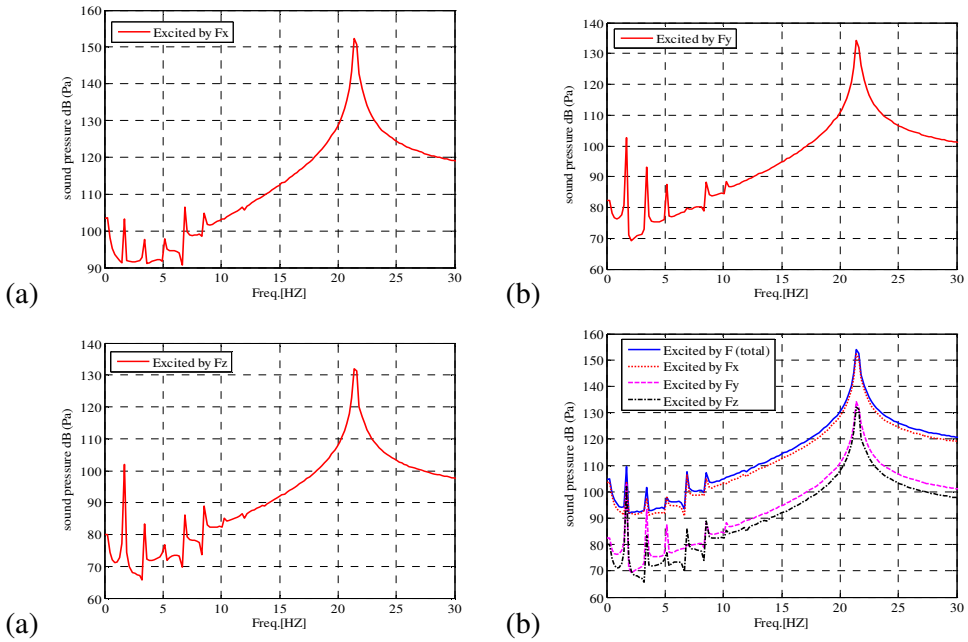

Figure 13. Sound pressure for near field point in plane x=0 at distance D_s down the propeller centre. (a) thrust excited (b) vertical force excited (c) transverse force excited (d) total force excited.

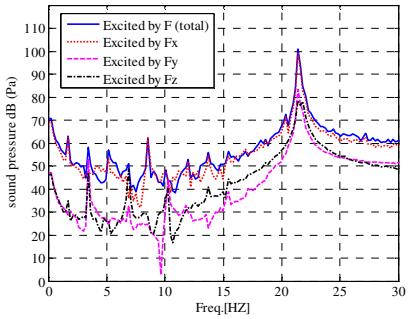

Figure 14. Sound pressure for far field point in plane x=0 at distance $10D_s$ down the propeller centre.

Related to the acoustic response due to the exciting force, however all publications in this field figure out the acoustic response only at the PBF and its multiplications. But through this new method, it becomes available to figure out the response at n_s and its multiplications. The results in Figure 13 and Figure 14 for the near and far field respectively show that, the SPL due to the applied force in single direction or the total forces of all directions at n_s and its harmonies are quite near or higher than SPL at the BPF. This means that the response at these new harmonies could not be avoided, and this is the first contribution of this work. On the other hand, the figures show very important and new thing that, the sound pressure is mainly tonal at the structural fundamental frequency, and the maximum value of the radiated sound pressure is occurred at 21.58 Hz. This means that, the contribution of the propeller structural modes in underwater acoustic response are more important than the contribution at the propeller operating speed and its harmonies, and this is the second contribution of this work. The results also show that, SPL induced due to the thrust force is the maximum one among the forces in the other two directions, almost the same SPL induced due to the total forces as shown in Figure 13(d) and Figure 14.

8. Conclusion

This new method considered two new important parameters, the 1st one is the applying of the exciting forces due to the propeller-ship interaction on the propeller surface as a distributed load, the 2nd one is the consideration of the propeller as 3-D structure. So, some new contributions are appeared as follows:
(1) The structural and acoustic responses at the propeller rotating speed and structural fundamental mode are higher than that at BPF. (2) The maximum value of the radiated sound pressure is happened not due to the harmonies of the exciting forces but due to the structural modes. (3) Related to the acoustic responses due to the exciting forces, the highest value of the SPL is at the 1st harmony of the propeller rotating speed among all the harmonies of the exciting force including the BPF. So, propeller rotating speed plays a major role in the sound radiation of the propulsion system more than the role at BPF. (4) The sounds pressure radiated due to the vertical and transverse forces are small compared with the radiated one due to thrust force which almost the same sound pressure radiated due to total forces.

REFERENCES

1 Wei Ying-San, Wang Yong-Sheng, Chang Shu-Ping, Fu Jian. Numerical prediction of propeller excited acoustic response of submarine structure based on CFD, FEM and BEM, *Journal of Hydrodynamics*, **24**(2), 207-216, (2012).

2 Wei Ying-San, Wang Yong-Sheng. Unsteady hydrodynamics of blade forces and acoustic responses of a model scaled submarine excited by propeller's thrust and side-forces, *Journal of Sound and Vibration*, **332**,2038 -2056, (2013)

3 Liao-Yuan Li, Yi-Peng Cao, Wen-Ping Zhang, Jia-You Yang. Research on propeller-induced ship hull vibration and underwater radiation noise, ICMT, Harbin, China, 25-28 June, (2012).

4 Yi-peng Cao, Liao-yuan Li, Xiu-zhen Ma. Study on underwater noise characteristics of ship structure induced by propeller exciting force, Internoise, Innsbruck, Austria, 15-18 September, (2013).

5 Singiresu S. Rao, Mechanical Vibrations, Fifth edition, Pearson, (2011).